AIP Advances

Effect of electromechanical coupling on locally resonant quasiperiodic metamaterials

Cite as: AIP Advances **13**, 015112 (2023); https://doi.org/10.1063/5.0119914
Submitted: 19 September 2022 • Accepted: 22 December 2022 • Published Online: 09 January 2023

Joshua LeGrande, Mohammad Bukhari and Oumar Barry

openaccess
View Online
Export Citation
CrossMark

AIP Publishing

© 2023 Author(s).

Effect of electromechanical coupling on locally resonant quasiperiodic metamaterials

Cite as: AIP Advances 13, 015112 (2023); doi: 10.1063/5.0119914
Submitted: 19 September 2022 • Accepted: 22 December 2022 •
Published Online: 9 January 2023

View Online Export Citation CrossMark

Joshua LeGrande, Mohammad Bukhari, and Oumar Barry[a)]

AFFILIATIONS

Vibrations and Robotics Lab, Department of Mechanical Engineering, Virginia Polytechnic Institute and State University, Blacksburg, Virginia 24061, USA

[a)]Author to whom correspondence should be addressed: obarry@vt.edu

ABSTRACT

Electromechanical metamaterials have been the focus of many recent studies for use in simultaneous energy harvesting and vibration control. Metamaterials with quasiperiodic patterns possess many useful topological properties that make them a good candidate for study. However, it is currently unknown what effect electromechanical coupling may have on the topological bandgaps and localized edge modes of a quasiperiodic metamaterial. In this paper, we study a quasiperiodic metamaterial with electromechanical resonators to investigate the effect on its bandgaps and localized vibration modes. We derive here the analytical dispersion surfaces of the proposed metamaterial. A semi-infinite system is also simulated numerically to validate the analytical results and show the band structure for different quasiperiodic patterns, load resistors, and electromechanical coupling coefficients. The topological nature of the bandgaps is detailed through an estimation of the integrated density of states. Furthermore, the presence of topological edge modes is determined through numerical simulation of the energy harvested from the system. The results indicate that quasiperiodic metamaterials with electromechanical resonators can be used for effective energy harvesting without changes in the bandgap topology for weak electromechanical coupling.

© 2023 Author(s). All article content, except where otherwise noted, is licensed under a Creative Commons Attribution (CC BY) license (http://creativecommons.org/licenses/by/4.0/). https://doi.org/10.1063/5.0119914

I. INTRODUCTION

Mechanical metamaterials are a novel class of artificially structured materials with valuable dynamic properties for vibration control and energy harvesting.[1] Periodic and locally resonant metamaterials are especially useful for their ability to produce bandgaps in their bulk spectra at wavelengths near the lattice constant for periodic structures[2–6] and at wavelengths much shorter than the lattice constant for locally resonant structures.[7–10] In the frequency range of these bandgaps, waves cannot propagate and are reflected due to the Bragg scattering.

More recent work has focused on using these metamaterials for simultaneous vibration control and energy harvesting through the introduction of electromechanical elements such as piezoelectric patches.[11–14] It has been shown that the presence of weak electromechanical coupling does not alter the bulk spectrum,[15,16] and tuning of a shunt circuit has proven effective in tuning bandgaps in the bulk spectrum.[17–20] Various methods have also been explored to increase the energy harvesting performance of these metamaterials such as using graded patterns in shunt circuits[21] and physically coupling resonators.[22]

Quasiperiodic metamaterials exhibit many useful topological properties that make them worthy of consideration for greater energy harvesting performance. Although periodic metamaterials produce topologically trivial bandgaps, quasiperiodic metamaterials can produce additional bandgaps that are topological in that they are filled with topological edge modes.[23,24] When plotted, the bulk spectrum has been shown analytically and experimentally to map the Hofstadter butterfly spectrum.[25–27] For finite structures, the topological edge modes filling the gaps in the bulk spectrum manifest through vibrations that are localized to the boundary of the structure.[25,28,29] Through the introduction of a phase variable to the pattern function, the edge modes can be pumped from one boundary to the other.[29] These topological edge modes allow for more effective energy harvesting as only the few cells with large amplitude vibrations will need energy harvesters embedded in them. However, the effect of the electromechanical coupling on the topological bandgaps and edge modes of a quasiperiodic structure remains

© Author(s) 2023

elusive to date. Therefore, detailing this effect is the focus of this study.

In this paper, we consider a 1D quasiperiodic chain of identical masses with electromechanical resonators. The quasiperiodic pattern is present through a variation in the spring stiffness between cells. The electromechanical resonators are shunted to an external load resistor for harvesting the generated power. The governing equations are presented, and the bulk spectrum is determined analytically for an infinite system and numerically for a semi-infinite system. The topological nature of the bandgaps is confirmed through the estimation of the integrated density of states (IDS). The effects of electromechanical coupling parameters on the topological bandgaps and edge modes are also observed. Furthermore, a discussion on the application of topological edge modes for use in energy harvesting is given with the power output from each cell in a semi-infinite chain.

II. SYSTEM DESCRIPTION AND MODELING

A schematic of the quasiperiodic structure under consideration is shown in Fig. 1(a). The structure consists of s equally spaced crystals of mass m and lattice constant a. Within each cell is embedded an electromechanical resonator shunted to an external resistor R. The electromechanical resonator has an effective mass m_p, effective stiffness k_p, electromechanical coupling coefficient θ, and capacitance of the piezoelectric element C_p. Each cell is connected by springs whose stiffness constant k_n is defined by the sampling of the 2D surface $S(x,\phi) = \cos(2\pi Qx + \phi)$ at $x_n = na$ [Fig. 1(b)], which is topologically equivalent[23] to the circle $\mathbb{S}^1$. This surface is defined by the quasiperiodic parameter Q and the phase variable ϕ. As such, the nth spring constant is defined as

$$k_n = k_0[1 + \alpha\cos(2\pi Qn + \phi)], \tag{1}$$

with average stiffness k_0 and modulation amplitude α. The governing equations of motion for the nth mass and electromechanical resonator are

$$m\ddot{u}_n + (k_{n-1} + k_n)u_n - k_{n-1}u_{n-1} - k_n u_{n+1} + m_p(\ddot{y}_n + \ddot{u}_n) = 0, \tag{2}$$

$$m_p\ddot{y}_n + k_p y_n - \theta v_n = -m_p\ddot{u}_n, \tag{3}$$

$$RC_p\dot{v}_n + v_n + R\theta\dot{y}_n = 0, \tag{4}$$

where $y_n = Y_n - u_n$ is the relative displacement of the nth resonator, Y_n is the absolute displacement of the nth resonator, u_n is the displacement of the nth cell, and v_n is the harvested voltage across the resistor.

Imposing a Bloch periodic solution of

$$u_n = \tilde{U}_n e^{j(\mu n - \omega t)} \quad y_n = \tilde{Y}_n e^{j(\mu n - \omega t)} \quad v_n = \tilde{V}_n e^{j(\mu n - \omega t)}, \tag{5}$$

where $\tilde{U}_n$, $\tilde{Y}_n$, and $\tilde{V}_n$ are the mass displacement, resonator displacement, and voltage amplitudes, respectively, with non-dimensional wavenumber μ, frequency ω, and dimensional time t, will yield the governing equations,

$$(-m\omega^2 + k_{n-1} + k_n)\tilde{U}_n - k_{n-1}\tilde{U}_{n-1}e^{-j\mu} - k_n\tilde{U}_{n+1}e^{j\mu} - m_p\omega^2\tilde{Y}_n = 0, \tag{6}$$

$$(-m_p\omega^2 + k_p)\tilde{Y}_n - k_p\tilde{U}_n - \theta\tilde{V}_n = 0, \tag{7}$$

$$\left(-j\omega + \frac{1}{RC_p}\right)\tilde{V}_n - j\omega\frac{\theta}{C_p}\tilde{Y}_n + j\omega\frac{\theta}{C_p}\tilde{U}_n = 0. \tag{8}$$

By further imposing the condition $u_{n+N} = u_n$ for a system with N masses in its unit cell, the governing equations for the unit cell can be expressed in matrix form as follows:

$$\begin{bmatrix} \mathbf{K} & -m_p\omega^2\mathbf{I}_N & \mathbf{0}_N \\ -k_p\mathbf{I}_N & (-m_p\omega^2 + k_p)\mathbf{I}_N & -\theta\mathbf{I}_N \\ j\omega\frac{\theta}{C_p}\mathbf{I}_N & -j\omega\frac{\theta}{C_p}\mathbf{I}_N & \left(-j\omega + \frac{1}{RC_p}\right)\mathbf{I}_N \end{bmatrix}\begin{bmatrix}\tilde{\mathbf{U}}\\ \tilde{\mathbf{Y}}\\ \tilde{\mathbf{V}}\end{bmatrix} = \mathbf{0}, \tag{9}$$

where the $N \times N$ stiffness matrix $\mathbf{K}$ can be expressed as

$$\mathbf{K} = -m\omega^2\mathbf{I}_N + \begin{bmatrix} k_N + k_i & -k_i e^{j\mu} & 0 & \dots & -k_N e^{-j\mu} \\ -k_{i-1}e^{-j\mu} & k_{i-1} + k_i & -k_i e^{j\mu} & \dots & 0 \\ 0 & \ddots & \ddots & \ddots & \vdots \\ \vdots & 0 & \ddots & \ddots & -k_{N-1}e^{j\mu} \\ -k_N e^{j\mu} & 0 & \dots & -k_{N-1}e^{-j\mu} & k_{N-1} + k_N \end{bmatrix}, \tag{10}$$

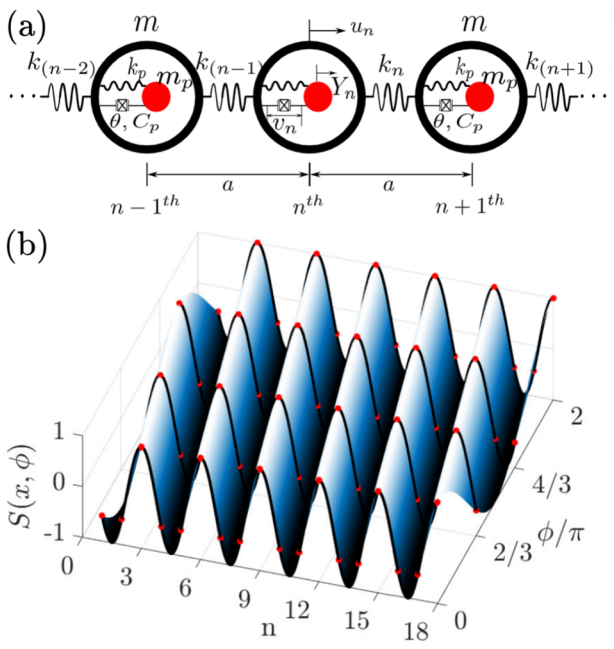

FIG. 1. (a) Schematic of the quasiperiodic metamaterial with electromechanical resonators. (b) 2D surface sampled at red dots along black lines of constant phase ϕ.

© Author(s) 2023

with i being the row number, and $\mathbf{I}_N$ and $\mathbf{0}_N$ being the $N \times N$ identity and zero matrices, respectively.

To obtain nontrivial solutions to Eq. (9), the coefficient matrix must be singular. By setting the determinant of the coefficient matrix equal to zero, the characteristic equation is obtained through which the analytical dispersion relationship is determined. With both the coefficient and stiffness matrices generalized for any value of N, this relationship can be applied to any rational quasiperiodic parameter value.

For this study, we will be giving further analytical consideration to a system with quasiperiodic parameter $Q = 1/3$ ($N = 3$) with stiffness matrix (see supplementary material for more details on other parameters)

$$\mathbf{K} = \begin{bmatrix} -m\omega^2 + k_1 + k_3 & -k_1 e^{j\mu} & -k_3 e^{-j\mu} \\ -k_1 e^{-j\mu} & -m\omega^2 + k_1 + k_2 & -k_2 e^{j\mu} \\ -k_3 e^{j\mu} & -k_2 e^{-j\mu} & -m\omega^2 + k_2 + k_3 \end{bmatrix}. \quad (11)$$

Numerical simulation is used to determine the natural frequencies and mode shapes for a semi-infinite system for the full range of phase variable ϕ and quasiperiodic parameter Q.

The topological nature of the bandgaps can also be classified through the estimation of the integrated density of states (IDS) of the system. This can be calculated at a frequency Ω as

$$\mathrm{IDS}(\Omega) = \lim_{s\to\infty} \frac{\sum_n [\omega_n \le \Omega]}{s}, \quad (12)$$

where ω_n is the nth natural frequency and $[\cdot]$ are the Iverson Brackets returning a value of 1 when the statement within is true and a value of 0 otherwise.

Next, the relative power output P_n from each cell is determined from the voltage mode shapes. The mode shape yields a relative voltage at each cell from which the instantaneous power can be derived using the following relation:

$$P_n = \frac{v_n^2}{R}. \quad (13)$$

III. EFFECT ON BAND STRUCTURE

Here, we will consider a semi-infinite chain of $s = 60$ masses and resonators with the following parameters: $m = 1$ kg, $k_0 = 1$ N/m, $\alpha = 0.6$, $m_p = 0.2$ kg, $k_p = 0.3$ N/m, $\phi = 0$ rad, $R = 10$ MΩ, $C_p = 13.3$ nF, and $\theta = 10^{-10}$ N/V. After calculating the roots of the characteristic equation derived from Eq. (9), we plot the dispersion surfaces in Fig. 2(a), showing six bulk bands and five bandgaps. To validate the analytical results, we also plot the natural frequencies of the semi-finite chain superimposed on the bulk bands in Fig. 2(b). The non-dimensional frequency is defined as $\Omega = \omega/\omega_0$, where $\omega_0^2 = k_0/m$.

The results indicate that weak electromechanical coupling has no noticeable effect on the shape of the band structure producing an identical band structure to the case without coupling, which is not included here for brevity. For comparison, these results are included in the supplementary material. The bulk spectrum is split into two major branches separated by a bandgap centered around the resonant frequency of the local resonators, $\Omega = 1.22$. Both branches are further divided by multiple additional bandgaps determined by the value of the quasiperiodic parameter. Each of these additional bandgaps is spanned by a topological edge mode highlighted in red in Fig. 2(b). These modes are a prominent feature of the semi-infinite system. As the phase varies, these edge modes span the bandgap from one bulk boundary to the next. As it touches the next boundary, the localized vibration transitions from one edge to another.

To further investigate the effect of the electromechanical coupling on the band structure, we plot the natural frequencies again for the semi-infinite chain superimposed on an approximate infinite chain while varying the quasiperiodic parameter in Fig. 3. Both weak and strong electromechanical couplings show the well-known Hofstadter butterfly image. For weak electromechanical coupling ($\theta = 10^{-10}$ N/V), the band structure is obtained for a range of resistance values of $10\ \Omega \le R \le 10^{10}\ \Omega$. The band structures produced matched the structure without coupling,[28] showing no impact due to weak coupling. Further results for other values of the resistance and coupling coefficient are included in the supplementary material. This demonstrates that with weak electromechanical coupling, a quasiperiodic metamaterial can be used for simultaneous energy harvesting and vibration suppression without degrading its bandgap boundaries.

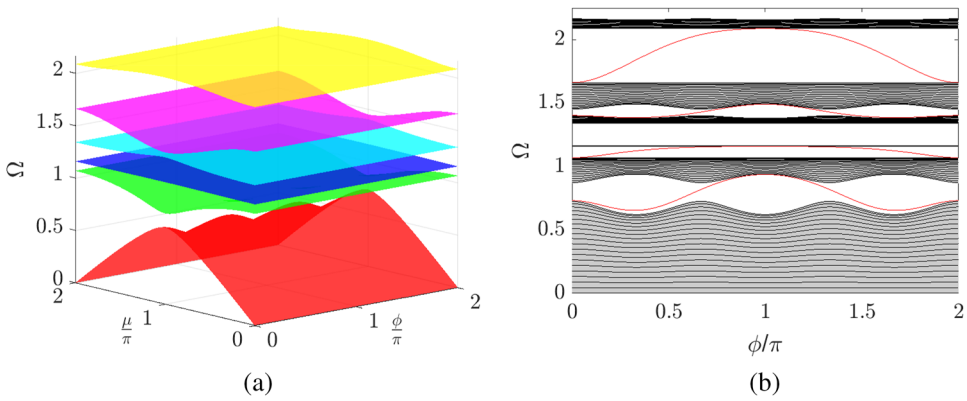

FIG. 2. (a) Dispersion surfaces as a function of μ and ϕ. (b) Natural frequencies for a chain of $s = 60$ cells (black lines) superimposed on bulk bands (shaded gray) with variation in the phase variable ϕ and $Q = 1/3$.

© Author(s) 2023

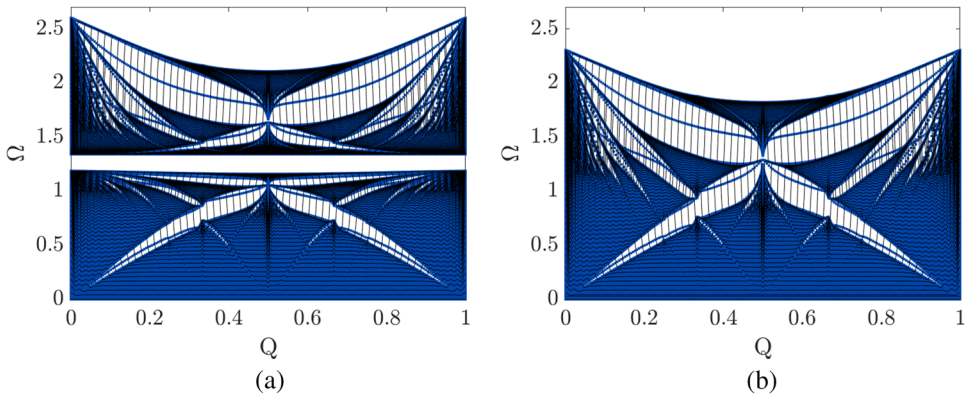

FIG. 3. Spectrum of natural frequencies for a chain of $s = 60$ cells (black lines) superimposed over a bulk spectrum of $s = 600$ cells (shaded blue) with (a) weak coupling ($\theta = 10^{-10}$ N/V) and (b) strong coupling ($\theta = 10^{-3}$ N/V) with variation in the quasiperiodic parameter Q and $\phi = 0$.

To test the case of stronger electromechanical coupling, the band structure was obtained for a range of coupling coefficients of 10^{-10} N/V $\leq \theta \leq 10^{-1}$ N/V. The band structure remains unaltered for $\theta \leq 10^{-5}$ N/V. As the coupling increases past this limit, the band structure gradually degrades. This is seen in Fig. 3(b), where multiple branches have merged as the bandgaps have collapsed. Indeed, this topological change in the spectrum is worthy of further investigation; however, it is beyond the scope of the current work, and we will consider it in the near future. It is worth noting that in most engineering applications, it is uncommon for the coupling coefficient to exceed the order of 10^{-10} N/V.

The topological nature of the bandgaps can be further detailed through the IDS function of the system. The IDS is plotted in Fig. 4 as a function of Ω and Q for an infinite system approximated with $s = 600$ cells with weak electromechanical coupling. The IDS is plotted for stronger coupling in the supplementary material. In this representation, the bandgaps are illustrated as lines along sharp color changes, some of which are traced as dashed lines in the figure. These lines can be defined as

$$\mathrm{IDS}(Q) = A + BQ, \tag{14}$$

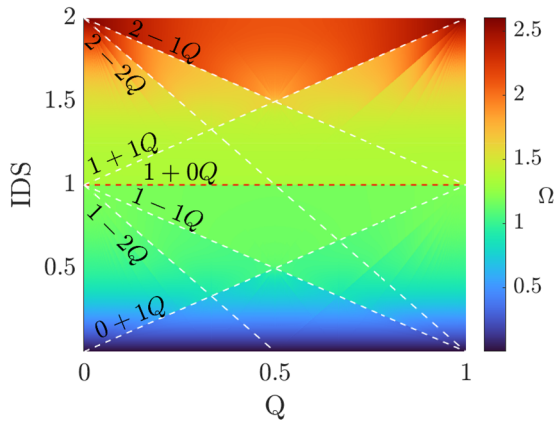

FIG. 4. Integrated density of states as a function of Q with sharp changes in color showing bandgaps. Some bandgaps are highlighted by dashed lines with their equations given.

with intercept A and slope B. Each bandgap can be uniquely labeled by its topological invariant, the Chern number, C. The IDS can be utilized to determine the Chern number using Streda's formula following the approach outlined by Ni *et al.*,[25] $\frac{\partial IDS}{\partial Q} = C$. From this approach, the slope B of each line indicates the Chern number used to define each associated bandgap and to determine the presence of topological edge modes. In Fig. 4, the red dashed line corresponds to the bandgap of the local resonators and has a Chern number (slope) $C = 0$ ($B = 0$), indicating it is topologically trivial. All other bandgaps are confirmed to be topological in that they have non-zero Chern numbers (slopes), which further implies the presence of topological edge modes spanning the bandgaps.

By exciting the system at the mode within the fifth bandgap and plotting the normalized power output, the presence of edge modes is made evident. Figure 5 shows the power output from each cell. The majority of the power output comes from only a handful of cells experiencing greater vibration in the localized mode. These few cells harvest energy that is multiple orders of magnitude larger than the majority of the remaining cells. By sweeping the phase variable, it is possible to shift the edge mode from one boundary to the other allowing for greater control of the location of vibration and energy harvesting in the chain. As such, the electromechanical coupling does not impact the ability of a quasiperiodic system to host localized edge modes. Furthermore, localized edge modes pave the way

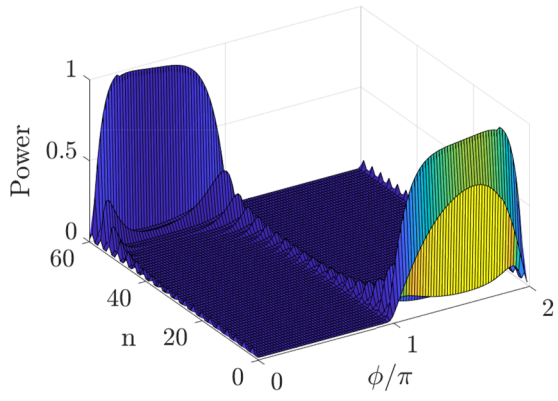

FIG. 5. Normalized power output from each cell in a chain of $s = 60$ cells.

© Author(s) 2023

for more efficient energy harvesting. With only a small portion of the cells participating in large relative vibration, only a few piezoelectric resonators are needed to harvest the majority of the energy in the system.

IV. CONCLUSION

In summary, we investigate the effect of energy harvesting on the topological bandgaps and edge modes of a locally resonant quasiperiodic metamaterial. The system under consideration was represented by a semi-infinite chain of spring-mass elements with variation in the spring constants following a quasiperiodic pattern. Each cell is connected to an electromechanical resonator modeled as a spring-mass system and shunted to a load resistor. Analytical dispersion surfaces are derived for an infinite system and validated numerically for a semi-infinite system. The bulk spectrum of the semi-infinite system is determined for a full range of phase variables and quasiperiodic parameters. It is also tested for different load resistors and electromechanical coupling values. The results show that quasiperiodic metamaterials with local resonance can be used to harvest energy without changing the topology of the bandgaps in the case of weak electromechanical coupling. However, the very strong coupling can degrade the performance as the band structure deforms and bandgaps collapse. The electromechanical coupling also has no negative impact on the topological edge modes spanning the bandgaps. With this consideration, it is feasible to design quasiperiodic metastructures for greater efficiency, which only require electromechanical energy harvesters on a small number of the total cells.

SUPPLEMENTARY MATERIAL

See supplementary material for further band structure results with various quasiperiodic parameters, load resistances, and electromechanical coupling as well as for discussion of vibration localization in other bandgaps.

ACKNOWLEDGMENTS

This work was supported in part by the National Science Foundation (NSF) Grant CMMI-2038187.

AUTHOR DECLARATIONS

Conflict of Interest

The authors have no conflicts to disclose.

Author Contributions

Joshua LeGrande: Formal analysis (lead); Investigation (lead); Methodology (equal); Writing – original draft (lead); Writing – review & editing (equal). **Mohammad Bukhari**: Conceptualization (equal); Funding acquisition (equal); Methodology (equal); Supervision (equal); Writing – review & editing (equal). **Oumar Barry**: Conceptualization (equal); Funding acquisition (equal); Project administration (lead); Supervision (equal); Writing – review & editing (equal).

DATA AVAILABILITY

The data that support the findings of this study are available from the corresponding author upon reasonable request.

REFERENCES

[1]M. I. Hussein, M. J. Leamy, and M. Ruzzene, "Dynamics of phononic materials and structures: Historical origins, recent progress, and future outlook," Appl. Mech. Rev. **66**, 040802 (2014).
[2]M. M. Sigalas and E. N. Economou, "Elastic and acoustic wave band structure," J. Sound Vib. **158**, 377–382 (1992).
[3]M. Sigalas and E. N. Economou, "Band structure of elastic waves in two dimensional systems," Solid State Commun. **86**, 141–143 (1993).
[4]M. S. Kushwaha, P. Halevi, L. Dobrzynski, and B. Djafari-Rouhani, "Acoustic band structure of periodic elastic composites," Phys. Rev. Lett. **71**, 2022 (1993).
[5]M. S. Kushwaha, P. Halevi, G. Martínez, L. Dobrzynski, and B. Djafari-Rouhani, "Theory of acoustic band structure of periodic elastic composites," Phys. Rev. B **49**, 2313 (1994).
[6]J. O. Vasseur, B. Djafari-Rouhani, L. Dobrzynski, M. S. Kushwaha, and P. Halevi, "Complete acoustic band gaps in periodic fibre reinforced composite materials: The carbon/epoxy composite and some metallic systems," J. Phys.: Condens. Matter **6**, 8759 (1994).
[7]Z. Liu, X. Zhang, Y. Mao, Y. Y. Zhu, Z. Yang, C. T. Chan, and P. Sheng, "Locally resonant sonic materials," Science **289**, 1734–1736 (2000).
[8]L. Liu and M. I. Hussein, "Wave motion in periodic flexural beams and characterization of the transition between Bragg scattering and local resonance," J. Appl. Mech. **79**, 011003 (2012).
[9]G. Huang and C. Sun, "Band gaps in a multiresonator acoustic metamaterial," J. Vib. Acoust. **132**, 031003 (2010).
[10]R. Zhu, X. N. Liu, G. K. Hu, C. T. Sun, and G. L. Huang, "A chiral elastic metamaterial beam for broadband vibration suppression," J. Sound Vib. **333**, 2759–2773 (2014).
[11]Y. Li, E. Baker, T. Reissman, C. Sun, and W. K. Liu, "Design of mechanical metamaterials for simultaneous vibration isolation and energy harvesting," Appl. Phys. Lett. **111**, 251903 (2017).
[12]N. E. Dutoit, B. L. Wardle, and S.-G. Kim, "Design considerations for MEMS-scale piezoelectric mechanical vibration energy harvesters," Integr. Ferroelectr. **71**, 121–160 (2005).
[13]G. Hu, L. Tang, A. Banerjee, and R. Das, "Metastructure with piezoelectric element for simultaneous vibration suppression and energy harvesting," J. Vib. Acoust. **139**, 011012 (2017).
[14]G. Hu, L. Tang, and R. Das, "Metamaterial-inspired piezoelectric system with dual functionalities: Energy harvesting and vibration suppression," in *Active and Passive Smart Structures and Integrated Systems 2017* (International Society for Optics and Photonics, 2017), Vol. 10164, p. 101641X.
[15]M. A. Bukhari, F. Qian, O. R. Barry, and L. Zuo, "Effect of electromechanical coupling on locally resonant metastructures for simultaneous energy harvesting and vibration attenuation applications," in *Dynamic Systems and Control Conference* (American Society of Mechanical Engineers (ASME), 2020), Vol. 84287, p. V002T38A003.
[16]M. Bukhari and O. Barry, "Simultaneous energy harvesting and vibration control in a nonlinear metastructure: A spectro-spatial analysis (vol 473, 115215, 2020)," J. Sound Vib. **487**, 115621 (2020).
[17]K. Yi and M. Collet, "Broadening low-frequency bandgaps in locally resonant piezoelectric metamaterials by negative capacitance," J. Sound Vib. **493**, 115837 (2021).
[18]F. Casadei, T. Delpero, A. Bergamini, P. Ermanni, and M. Ruzzene, "Piezoelectric resonator arrays for tunable acoustic waveguides and metamaterials," J. Appl. Phys. **112**, 064902 (2012).
[19]O. Thorp, M. Ruzzene, and A. Baz, "Attenuation and localization of wave propagation in rods with periodic shunted piezoelectric patches," Smart Mater. Struct. **10**, 979 (2001).

© Author(s) 2023

[20] A. Bergamini, T. Delpero, L. D. Simoni, L. D. Lillo, M. Ruzzene, and P. Ermanni, "Phononic crystal with adaptive connectivity," Adv. Mater. **26**, 1343–1347 (2014).
[21] M. Alshaqaq and A. Erturk, "Graded multifunctional piezoelectric metastructures for wideband vibration attenuation and energy harvesting," Smart Mater. Struct. **30**, 015029 (2020).
[22] G. Hu, L. Tang, and R. Das, "Internally coupled metamaterial beam for simultaneous vibration suppression and low frequency energy harvesting," J. Appl. Phys. **123**, 055107 (2018).
[23] D. J. Apigo, K. Qian, C. Prodan, and E. Prodan, "Topological edge modes by smart patterning," Phys. Rev.Mater. **2**, 124203 (2018).
[24] D. J. Apigo, W. Cheng, K. F. Dobiszewski, E. Prodan, and C. Prodan, "Observation of topological edge modes in a quasiperiodic acoustic waveguide," Phys. Rev. Lett. **122**, 095501 (2019).
[25] X. Ni, K. Chen, M. Weiner, D. J. Apigo, C. Prodan, A. Alu, E. Prodan, and A. B. Khanikaev, "Observation of Hofstadter butterfly and topological edge states in reconfigurable quasi-periodic acoustic crystals," Commun. Phys. **2**, 55 (2019).
[26] R. K. Pal, M. I. N. Rosa, and M. Ruzzene, "Topological bands and localized vibration modes in quasiperiodic beams," New J. Phys. **21**, 093017 (2019).
[27] Y. Xia, A. Erturk, and M. Ruzzene, "Topological edge states in quasiperiodic locally resonant metastructures," Phys. Rev. Appl. **13**, 014023 (2020).
[28] A. Glacet, A. Tanguy, and J. Réthoré, "Vibrational properties of quasi-periodic beam structures," J. Sound Vib. **442**, 624–644 (2019).
[29] M. I. N. Rosa, R. K. Pal, J. R. F. Arruda, and M. Ruzzene, "Edge states and topological pumping in spatially modulated elastic lattices," Phys. Rev. Lett. **123**, 034301 (2019).

© Author(s) 2023